

# LLR-Based Successive Cancellation List Decoding of Polar Codes

Alexios Balatsoukas-Stimming, *Student Member, IEEE*, Mani Bastani Parizi, *Student Member, IEEE*,  
and Andreas Burg, *Member, IEEE*

**Abstract**—Successive cancellation list decoding is a variant of Arikan’s conventional successive cancellation decoder for polar codes which enhances their finite-length performance in terms of the error probability. In this work, we show that successive cancellation list decoding can be formulated using log-likelihood ratios, which are numerically stable and lead to more efficient hardware implementations compared to the existing log-likelihood based implementations. Moreover, the log-likelihood ratio based formulation has some useful properties which allow us to significantly simplify the metric sorting step involved in successive cancellation list decoding. These improvements enable the design of a log-likelihood ratio based decoder architecture which has up to 220% higher throughput per unit area than existing architectures. To the best of our knowledge, this is the successive cancellation list decoder architecture with the best hardware efficiency so far reported in the literature.

**Index Terms**—Successive Cancellation List Decoder, Polar Codes, Hardware Implementation

## I. INTRODUCTION

IN his seminal work [1], Arikan showed that it is possible to transform  $N$  independent copies of a noisy binary-input discrete memoryless channel (B-DMC), into  $N$  ‘easy-to-use’ synthetic B-DMCs; these B-DMCs are either almost noiseless (i.e., the input can be reliably decoded given the output) or useless (i.e., the output is statistically independent of the input). In other words, the synthetic channels *polarize*. More importantly, the fraction of noiseless synthetic channels approaches the symmetric capacity of the original channel. Based on the channel polarization phenomenon, *polar codes* are constructed by sending uncoded data bits through the noiseless synthetic channels. The receiver can decode the data bits reliably *and efficiently* using a successive cancellation (SC) decoder. The SC decoder is attractive from an implementation perspective due to its highly structured nature. Consequently, several hardware architectures for SC decoding of polar codes have recently been presented in the literature [2], [3], [4], [5], [6], and the first SC decoder ASIC was presented in [7].

Despite the powerful asymptotic performance of polar codes, whose block-error probability under SC decoding decays roughly like  $O(2^{-\sqrt{N}})$  [8], polar codes do not perform

well at low-to-moderate block-lengths. This is to a certain extent due to the sub-optimality of the SC decoding algorithm. To partially compensate for this sub-optimality, Tal and Vardy proposed the successive cancellation list (SCL) decoder whose computational complexity is shown to scale identically to the SC decoder with respect to the block-length  $N$  [9].

The SCL algorithm in [9] is described in terms of likelihoods. Unfortunately, computations with likelihoods are numerically unstable as they are prone to underflows. In recent hardware implementations of the SCL decoder [10], [11], [12] the stability problem was solved by using log-likelihoods (LLs). However, the use of LLs creates other important problems, such as an irregular memory with varying word bit-width, as well as large processing elements (PEs) making these decoders still inefficient in terms of area and throughput.

**Contribution:** In this work, we prove that the SCL decoding algorithm can be formulated exclusively in the *log-likelihood ratio* (LLR) domain, thus enabling area-efficient and numerically stable implementation of SCL decoding. Moreover, the LLR-based implementation enables a significant reduction of the size of our previous hardware architecture [10], [13], as well as an increase of its maximum operating frequency. We also leverage some useful properties of the LLR-based formulation in order to reduce the complexity of the sorting step of SCL decoding. More specifically, these properties are used to *prune* the radix- $2L$  sorter used in [10], [13] by avoiding unnecessary comparisons. Besides the implementation gains, it is noteworthy that most processing blocks in practical receivers process the data in the form of LLRs. Therefore, the LLR-based SCL decoder can readily be incorporated into existing systems while the LL-based decoders would require extra processing stages to convert the channel LLRs into LLs.

**Outline:** The remainder of this paper is organized as follows. In Section II we review the theory of polar codes and discuss how the SCL decoder can improve the performance of the conventional SC decoder proposed by Arikan. Then, in Section III we formulate the SCL decoder in the LLR domain. Section IV reviews the SC decoder architecture on which our SCL decoder architecture, presented in Section V, is based, and in Section VI we see how the sorter can be simplified. We then present hardware synthesis results and compare our decoder with previously existing decoders of [10], [11] in Section VII. Finally, we discuss some open problems and potential further improvements of the presented decoder in Section VIII.

A. Balatsoukas-Stimming and A. Burg are with the Telecommunications Circuits Laboratory (TCL), EPFL. Their research is supported by the Swiss National Science Foundation grant 200021\_149447.

M. Bastani Parizi is with the Information Theory Laboratory (LTHI), EPFL. His research is supported by the Swiss National Science Foundation grant 200020\_146832.

This work has been published in parts in the 39th International Conference on Acoustics, Speech and Signal Processing (ICASSP’2014).

The authors would like to thank Professor Emre Telatar, Professor Ido Tal and Jun Lin for helpful discussions.

*Notation:* Throughout this paper, boldface letters denote vectors. The elements of a vector  $\mathbf{x}$  are denoted by  $x_i$ . By  $\mathbf{x}_l^m$  we mean the sub-vector  $[x_l, x_{l+1}, \dots, x_m]^T$  if  $m \geq l$  and the null vector otherwise. If  $\mathcal{I} = \{i_1, i_2, \dots\}$  is a set of indices such that  $i_1 < i_2 < \dots$ , then  $\mathbf{x}_{\mathcal{I}}$  denotes the sub-vector  $[x_{i_1}, x_{i_2}, \dots]^T$ . For  $a, b \in \mathbb{Z}$ ,  $[a : b]$  represents the set of integers  $\{a, a+1, \dots, b-1, b\}$ . If  $\mathcal{S}$  is a countable set,  $|\mathcal{S}|$  denotes its cardinality.  $\log(\cdot)$  and  $\ln(\cdot)$  denote based-2 and natural logarithm respectively.

## II. BACKGROUND

In this section, we briefly review Arkan's channel polarization theorem based on which polar codes are constructed. We then describe the SC decoding algorithms and discuss how the SCL decoder improves the performance of the conventional SC decoder.

### A. Channel Polarization

Let  $W : \mathcal{X} \rightarrow \mathcal{Y}$  be a B-DMC with input alphabet  $\mathcal{X} = \{0, 1\}$ , output alphabet  $\mathcal{Y}$  and transition probabilities  $W(y|x)$  (for  $\forall x \in \mathcal{X}$  and  $\forall y \in \mathcal{Y}$ ) whose symmetric capacity is

$$I(W) \triangleq \sum_{y \in \mathcal{Y}} \sum_{x \in \mathcal{X}} \frac{1}{2} W(y|x) \log \frac{W(y|x)}{\frac{1}{2}W(y|0) + \frac{1}{2}W(y|1)}.$$

The symmetric capacity is the highest rate at which reliable communication is possible through  $W$  if the input letters are used with equal frequency, and reflects how noisy the channel is.

For  $N = 2^n$ ,  $n \geq 1$ , let the binary vectors  $\mathbf{u} \in \mathcal{X}^N$  and  $\mathbf{x} \in \mathcal{X}^N$  be related through the linear transform

$$\mathbf{x} = \begin{bmatrix} 1 & 1 \\ 0 & 1 \end{bmatrix}^{\otimes n} \mathbf{B}_n \mathbf{u} \triangleq \mathbf{G}_n \mathbf{u}, \quad (1)$$

where  $\otimes n$  denotes the  $n$ -th Kronecker power of the matrix and  $\mathbf{B}_n$  is the bit-reversal permutation.<sup>1</sup> Suppose  $\mathbf{x}$  is the input to  $N$  independent copies of  $W$  resulting in  $\mathbf{y} \in \mathcal{Y}^N$  as the output. In other words, conditioned on  $\mathbf{X} = \mathbf{x}$ , the distribution of the random vector  $\mathbf{Y} \in \mathcal{Y}^N$  is

$$W^N(\mathbf{y}|\mathbf{x}) \triangleq \Pr[\mathbf{Y} = \mathbf{y}|\mathbf{X} = \mathbf{x}] = \prod_{i=0}^{N-1} W(y_i|x_i), \quad (2)$$

for  $\forall \mathbf{y} \in \mathcal{Y}^N, \mathbf{x} \in \mathcal{X}^N$ . Finally, let  $W_n : \mathcal{X}^N \rightarrow \mathcal{Y}^N$  denote the 'effective' channel seen from  $\mathbf{U}$  to  $\mathbf{Y}$ . That is,

$$W_n(\mathbf{y}|\mathbf{u}) \triangleq \Pr[\mathbf{Y} = \mathbf{y}|\mathbf{U} = \mathbf{u}] = W^N(\mathbf{y}|\mathbf{G}_n \mathbf{u}), \quad (3)$$

for  $\forall \mathbf{u} \in \mathcal{X}^N, \mathbf{y} \in \mathcal{Y}^N$  with  $W^N(\mathbf{y}|\mathbf{x})$  as in (2).

From the channel  $W_n : \mathcal{X}^N \rightarrow \mathcal{Y}^N$ , we 'synthesize'  $N$  B-DMCs,  $W_n^{(i)} : \mathcal{X} \rightarrow \mathcal{Y} \times \mathcal{X}^i$ ,  $i \in [0 : N-1]$ , as

$$W_n^{(i)}(\mathbf{y}, \mathbf{u}_0^{i-1}|u_i) \triangleq \sum_{\mathbf{u}_{i+1}^{N-1} \in \mathcal{X}^{N-i-1}} \frac{1}{2^{N-1}} W_n(\mathbf{y}|\mathbf{u}). \quad (4)$$

Namely,  $W_n^{(i)}$  is the B-DMC whose input is  $U_i$  and its output is the physical channel output  $\mathbf{Y}$  together with side

<sup>1</sup>Let  $\mathbf{v}$  and  $\mathbf{u}$  be two length  $N = 2^n$  vectors and index their elements using binary sequences of length  $n$ ,  $(b_1, b_2, \dots, b_n) \in \{0, 1\}^n$ . Then  $\mathbf{v} = \mathbf{B}_n \mathbf{u}$  iff  $v_{(b_1, b_2, \dots, b_n)} = u_{(b_n, b_{n-1}, \dots, b_1)}$  for  $\forall (b_1, b_2, \dots, b_n) \in \{0, 1\}^n$ .

information  $\mathbf{U}_0^{i-1}$  (all preceding elements of  $\mathbf{U}$ ) considering all the following elements of  $\mathbf{U}$  as random unknown bits.

Arkan's fundamental result [1, Theorem 1] states that as  $n \rightarrow \infty$ , for all except a vanishing fraction of indices  $i \in [0 : N-1]$ , either  $I(W_n^{(i)}) \approx 1$  (almost noiseless channels) or  $I(W_n^{(i)}) \approx 0$  (useless channel). Furthermore, a straightforward application of the chain rule for mutual information shows that  $\sum_{i=0}^{N-1} I(W_n^{(i)}) = NI(W)$ . Consequently, the fraction of the almost-noiseless channels is equal to the symmetric capacity of the underlying physical channel.

### B. Polar Coding

Having transformed  $N$  identical copies of a 'moderate' B-DMC  $W$  into  $N$  'extremal' B-DMCs (involving, in particular, approximately  $NI(W)$  noiseless channels) we can exploit these channels to transmit information bits. Since each synthetic channel  $W_n^{(i)}$  requires the input to *all* previous synthetic channels  $\mathbf{U}_0^{i-1}$  as side information (in addition to the physical channel output  $\mathbf{Y}$ ) by definition, the input of the useless channels should additionally be revealed to the decoder to guarantee that it can reliably decode the inputs of the noiseless channels. Having almost  $NI(W)$  noiseless channels implies such a transmission scheme will achieve the symmetric capacity of  $W$ .

1) *Polar Codes:* In order to construct a polar code of rate  $R$  and block length  $N$  for a channel  $W$ , the indices of  $NR$  synthetic channels  $W_n^{(i)}, i \in [0 : N-1]$  with highest symmetric capacity are selected as the *information* indices denoted by  $\mathcal{A} \subset [0 : N-1]$ . The sub-vector  $\mathbf{u}_{\mathcal{A}}$  will be set to the  $NR$  data bits to be sent to the receiver and  $\mathbf{u}_{\mathcal{F}}$  (where  $\mathcal{F} = [0 : N-1] \setminus \mathcal{A}$ ) is fixed to some *frozen* vector which is known to the receiver. The vector  $\mathbf{u}$  is then encoded to the codeword  $\mathbf{x}$  through (1) using  $O(N \log N)$  binary additions (cf. [1, Section VII]) and transmitted via  $N$  independent uses of the channel  $W$ .

2) *Successive Cancellation Decoder:* The receiver observes  $\mathbf{y}$  which is a noisy version of  $\mathbf{x}$  and estimates the elements of the sub-vector  $\mathbf{u}_{\mathcal{A}}$  *successively* as follows: Suppose the information indices are ordered as  $\mathcal{A} = \{i_1, i_2, \dots, i_{NR}\}$  (where  $i_j < i_{j+1}$ ). Having the channel output, the receiver has all the required information to decode the input of the synthetic channel  $W_n^{(i_1)}$  as  $\hat{u}_{i_1}$ . Since this synthetic channel is assumed to be almost-noiseless by construction,  $\hat{u}_{i_1} = u_{i_1}$  with high probability. Subsequently, the decoder can proceed to index  $i_2$  as the information required for decoding the input of  $W_n^{(i_2)}$  is now available. Once again, this estimation is with high probability error-free. This process is continued until all the information bits are estimated as formalized in Algorithm 1.

3) *SC Decoding as a Greedy Tree Search Algorithm:* Let

$$\mathcal{U}(\mathbf{u}_{\mathcal{F}}) \triangleq \{\mathbf{v} \in \mathcal{X}^N : \mathbf{v}_{\mathcal{F}} = \mathbf{u}_{\mathcal{F}}\} \quad (5)$$

denote the set of all possible  $2^{NR}$  vectors of length  $N$  that transmitter can send. The elements of  $\mathcal{U}(\mathbf{u}_{\mathcal{F}})$  are in one-to-one correspondence with  $2^{NR}$  leaves of a binary tree of height  $N$ : the leaves are constrained to be reached from the root by following the direction  $u_i$  at all levels  $i \in \mathcal{F}$ . Therefore, any

**Algorithm 1:** SC Decoding Algorithm [1].

---

```

1 for  $i = 0, 1, \dots, N - 1$  do
2   if  $i \notin \mathcal{A}$  then                               /* frozen bits */
3      $\hat{u}_i \leftarrow u_i$ ;
4   else                                           /* information bits */
5      $\hat{u}_i \leftarrow \arg \max_{u_i \in \{0,1\}} W_n^{(i)}(\mathbf{y}, \hat{\mathbf{u}}^{i-1} | u_i)$ ;
6 return  $\hat{\mathbf{u}}_{\mathcal{A}}$  ;

```

---

decoding procedure is essentially equivalent to picking a *path* from the root to one of these leaves on the binary tree.

In particular, the optimal ML decoder, associates each path with a ‘metric’ which is its likelihood (or any monotone function of its likelihood) and picks the path that maximizes this metric by exploring *all* possible paths:

$$\hat{\mathbf{u}}_{\text{ML}} = \arg \max_{\mathbf{v} \in \mathcal{U}(\mathbf{u}_{\mathcal{F}})} W_n(\mathbf{y} | \mathbf{v}).$$

Clearly such a maximization problem is computationally infeasible as there are exponentially many paths (with respect to the number of information bits  $NR$  in a block of  $N$  bits) to search through.

The SC decoder, in contrast, maximizes the metric in a *greedy* manner by performing a one-time-pass through the binary tree: starting from the root, at each level  $i \in \mathcal{A}$ , the decoder extends the existing path by picking the child that maximizes the *partial likelihood*  $W_n^{(i)}(\mathbf{y}, \hat{\mathbf{u}}_0^{i-1} | u_i)$ . This is clearly a sub-optimal solution. In return for this sub-optimality, we shall shortly see that the SC decoding is computationally efficient and, despite its sub-optimality its block-error probability decays roughly like  $O(2^{-\sqrt{N}})$  [8].

Note that if, instead of extending the existing path in only one direction, at each level  $i \in \mathcal{A}$ , the decoder could be duplicated into two parallel threads continuing in either possible direction, all  $2^{NR}$  possible paths could eventually be explored and their likelihoods would be computed ( $W_n^{(N-1)}(\mathbf{y}, \mathbf{u}^{N-2} | u_{N-1})$  is proportional to  $W(\mathbf{y} | \mathbf{u})$  as can be seen in (4)). Thus, an ML decoder could be realized by running exponentially many SC decoders in parallel.

4) *Complexity of the SC Decoder:* For the decisions of line 5 of Algorithm 1 the decoder needs to compute the pair of synthetic channel likelihoods  $W_n^{(i)}(\mathbf{y}, \hat{\mathbf{u}}^{i-1} | u_i)$ ,  $u_i \in \{0, 1\}$ . In this section, we review how these computations are done efficiently, leading to a total decoding complexity of  $O(N \log N)$  with the aim of setting up the terminology that we need for stating our main results.

The SC decoder decisions are binary for which the *decision log-likelihood ratios (LLRs)*,

$$L_n^{(i)} \triangleq \ln \frac{W_n^{(i)}(\mathbf{y}, \hat{\mathbf{u}}_0^{i-1} | 0)}{W_n^{(i)}(\mathbf{y}, \hat{\mathbf{u}}_0^{i-1} | 1)}, \quad i \in [0 : N - 1] \quad (6)$$

are sufficient statistics.

**Proposition 1.** *The decision LLRs,  $L_n^{(i)}$ ,  $i \in [0 : N - 1]$  can be computed via the recursions,*

$$\begin{aligned} L_s^{(2i)} &= f_- (L_{s-1}^{(2i-[i \bmod 2^{s-1}])}, L_{s-1}^{(2^s+2i-[i \bmod 2^{s-1}])}) \\ L_s^{(2i+1)} &= f_+ (L_{s-1}^{(2i-[i \bmod 2^{s-1}])}, L_{s-1}^{(2^s+2i-[i \bmod 2^{s-1}])}, u_s^{(2i)}) \end{aligned}$$

for  $s = n, n - 1, \dots, 1$ , where  $f_- : \mathbb{R}^2 \rightarrow \mathbb{R}$  and  $f_+ : \mathbb{R}^2 \times \mathcal{X} \rightarrow \mathbb{R}$  are defined as

$$f_-(\alpha, \beta) \triangleq \ln \frac{e^{\alpha+\beta} + 1}{e^\alpha + e^\beta}, \quad (8a)$$

$$f_+(\alpha, \beta, u) \triangleq (-1)^u \alpha + \beta, \quad (8b)$$

respectively. The recursions terminate at  $s = 0$  where

$$L_0^{(i)} \triangleq \ln \frac{W(y_i | 0)}{W(y_i | 1)}, \quad \forall i \in [0 : N - 1]$$

are channel LLRs. The partial sums  $u_s^{(i)}$  are computed starting from

$$u_n^{(i)} \triangleq \hat{u}_i, \quad \forall i \in [0 : N - 1]$$

and setting

$$u_{s-1}^{(2i-[i \bmod 2^{s-1}])} = u_s^{(2i)} \oplus u_s^{(2i+1)}, \quad (9a)$$

$$u_{s-1}^{(2^s+2i-[i \bmod 2^{s-1}])} = u_s^{(2i+1)}, \quad (9b)$$

for  $s = n, n - 1, \dots, 1$ .

Proposition 1 is a restatement of Arkan’s result in [1, Section VIII] in the LLR domain (instead of the likelihood-ratios) hence we do not prove it. It is clear that the entire set of  $N \log N$  LLRs  $L_s^{(i)}$ ,  $s \in [1 : \log N]$ ,  $i \in [0 : N - 1]$  can be computed using  $O(N \log N)$  updates since from each pair of LLRs at *stage*  $s$ , a pair of LLRs at stage  $s + 1$  are calculated using  $f_-$  and  $f_+$  update rules (cf. Figure 1). Additionally the decoder must keep track of  $N \log N$  partial sums  $u_s^{(i)}$ ,  $s \in [0 : n - 1]$ ,  $i \in [0 : N - 1]$  and update them after decoding each bit  $\hat{u}_i$ . Observe that since half of partial sums at stage  $s$  are just a repetition of a partial sum at stage  $s - 1$ , only  $\frac{N}{2} \log(N)$  distinct memory elements are sufficient to store the entire set of partial sums.

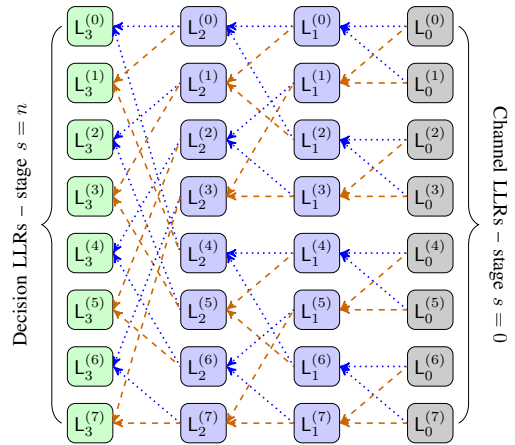


Fig. 1. The butterfly computational structure of the SC decoder for  $n = 3$ ; blue and orange arrows show  $f_-$  and  $f_+$  updates respectively.

It can be shown that the resulting partial sums at stage  $s = 0$  correspond to the output of a polar *encoder* whose input is  $\hat{\mathbf{u}}$ . That is  $u_0^{(i)} = \hat{x}_i$  where  $\hat{\mathbf{x}} = \mathbf{G}_n \hat{\mathbf{u}}$  (that is actually how the polar encoder implemented in using  $O(N \log N)$  additions).

*Remark.* It can be checked that (cf. [2])

$$f_-(\alpha, \beta) \approx \tilde{f}_-(\alpha, \beta) \triangleq \text{sign}(\alpha) \text{sign}(\beta) \min\{|\alpha|, |\beta|\}, \quad (10)$$

where  $\tilde{f}_-$  is a ‘hardware-friendly’ function as it involves only the easy-to-implement  $\min\{\cdot, \cdot\}$  operation (compared to  $f_-$  which involves exponentiations and logarithms). For a hardware implementation of the SC decoder the update rule  $f_-$  is replaced by  $\tilde{f}_-$ . Given  $f_+$ , such an approximation is called the “min-sum approximation” of the decoder.

### C. Successive Cancellation List Decoding

In Section II-B3 we saw that the optimal decoding problem can be solved by running exponentially many SC decoders in parallel. This is the main idea behind the *successive cancellation list (SCL)* decoding algorithm, introduced in [9], with the difference that, for maintaining an affordable computational complexity, the decoding is constrained to continue along only  $L$  parallel decoding threads.<sup>2</sup> To this end, except for the first  $\log(L)$  information bits, at each level step  $i \in \mathcal{A}$ , the likelihood of all  $2L$  tentative paths to continue are compared and the  $L$  most-likely of them are retained. This procedure is formalized in Algorithm 2. The block-error probability SCL decoding is reduced compared to SC decoding since, instead of performing a one-time-pass through the binary tree, it performs a breadth first search under a complexity constraint of exploring at most  $L$  paths in parallel (see [14, Figure 3] for an illustration).

---

#### Algorithm 2: SCL Decoding Algorithm [9]

---

```

1 for  $i = 0, 1, \dots, N - 1$  do
2   if  $i \notin \mathcal{A}$  then
3      $\hat{u}_i[\ell] \leftarrow u_i, \forall \ell \in [0 : L - 1]$ ;
4   else
5     if fewer than  $L$  paths are active then
6       foreach active path  $\ell$  do
7         Copy the thread  $\ell$  into a new thread  $\ell'$ ;
8          $\hat{u}_i[\ell] \leftarrow 0$ ;
9          $\hat{u}_i[\ell'] \leftarrow 1$ ;
10      else
11         $P_{\ell,u} \leftarrow W_n^{(i)}(\mathbf{y}, \hat{\mathbf{u}}^{i-1}[\ell]|u)$ , for  $\forall \ell \in [0 : L - 1]$ 
12        and  $\forall u \in \{0, 1\}$ ;
13         $\tau \leftarrow$  the median of  $2L$  numbers  $P_{\ell,u}$ ;
14        for  $\ell = 0, 1, \dots, L - 1$  do
15          if both  $P_{\ell,0} < \tau$  and  $P_{\ell,1} < \tau$  then
16            Eliminate the decoding thread  $\ell$ ;
17          else if  $P_{\ell,u} > \tau$  while  $P_{\ell,u \oplus 1} < \tau$  then
18             $\hat{u}_i[\ell] \leftarrow u$ ;
19          else
20            Copy the thread  $\ell$  into a new thread  $\ell'$ ;
21             $\hat{u}_i[\ell] \leftarrow 0$ ;
22             $\hat{u}_i[\ell'] \leftarrow 1$ ;
23  $\ell^* \leftarrow \arg \max_{\ell} W_n^{(N-1)}(\mathbf{y}, \hat{\mathbf{u}}^{N-1}[\ell]|\hat{u}_N[\ell])$ ;
24 return  $\hat{\mathbf{u}}_{\mathcal{A}}[\ell^*]$ ;

```

---

It is intuitively evident that as the list size  $L$  grows, the performance of the SCL decoder should get better. Simulation results in [9] show that for a block-length of  $N = 2048$  bits, a relatively small list size of  $L = 32$  is sufficient to have close-to-ML performance.

We conclude this section by a brief discussion about the complexity of SCL decoding. The entire decoding process

involves  $\Theta(L \cdot N)$  duplications (lines 7 and 19 of the algorithm) each of which requiring copying data structures of size  $\Omega(N)$ . Therefore, ignoring the complexity of the arithmetics, the complexity of decoding algorithm should scale at least as bad as  $\Omega(L \cdot N^2)$ . However, a clever choice of data structures, together with the recursive nature of the computations enables the authors of [9] to use a copy-on-write mechanism and implement the decoder in  $O(L \cdot N \log N)$  complexity.

### D. CRC-Aided Successive Cancellation List Decoder

The authors of [9] observe that when the SCL decoder fails, in most of the cases, the correct path (corresponding to  $\mathbf{u}_{\mathcal{A}}$ ) is among the  $L$  paths the list decoder has ended up with. The decoding error happens since there exists another more likely path which is selected in line 22 as the output of the decoder (note that in such situations the ML decoder would also fail). They, hence, conclude that the performance of polar codes would be significantly improved if the decoder were assisted for its final choice.

Such an assistance can be realized by adding  $r$  more non-frozen bits (i.e., creating a polar code of rate  $R + r/N$  instead of rate  $R$ ) to the underlying polar code and then setting the last  $r$  non-frozen bits to an  $r$ -bit CRC of the first  $NR$  information bits (note that the *effective* information rate of the code is unchanged). The SCL decoder, at line 22, first discards the paths that do not pass the CRC and then chooses the most-likely path among the remaining ones. Note that the CRC can be computed efficiently [15, Chapter 7]. The empirical results of [9] show that a modified polar code of block-length  $N = 2048$  and rate  $R = \frac{1}{2}$ , decoded using a list decoder with list size of  $L = 32$  and assisted with a 16-bit CRC, outperforms the existing state-of-the-art LDPC code of block-length  $N = 2304$  used in WiMAX standard at the same rate.

## III. LLR-BASED PATH METRIC COMPUTATION

Algorithms 1 and 2 are both valid high-level descriptions of SC and SCL decoding, respectively. However, for implementing these algorithms, the stability of the computations is crucial. Both algorithms we introduced in Section II are described in terms of likelihoods which are *not* safe quantities to work with; a decoder implemented using the likelihoods is prone to underflow errors as the likelihoods become tiny numbers.<sup>3</sup>

Recalling the binary tree picture that we provided in Section II-B3, the decision LLRs  $L_n^{(i)}$  (cf. (6)) summarize all the necessary information for choosing the most likely child among two children of the same parent at level  $i$ . In Section II-B4 we saw that having this type of decisions in the conventional SC decoder allows us to implement it in the LLR domain using numerically stable operations. However, in the SCL decoder, the problem is to choose  $L$  most likely children out of  $2L$  children of  $L$  different parents (lines 11 and 12 of Algorithm 2). For these kind of comparisons the decision LLRs  $L_n^{(i)}$  alone are not sufficient.

<sup>2</sup>Although it is not necessary,  $L$  is normally a power of 2.

<sup>3</sup>As noticed in [9], it is not difficult to see that  $W_n^{(i)}(\mathbf{y}, \mathbf{u}^{i-1}|u_i) \leq 2^{-i}$ .

Consequently, the software implementation of the decoder in [9] implements the decoder in the likelihood domain by rewriting the recursions of Proposition 1 for computing pairs of likelihoods  $W_n^{(i)}(\mathbf{y}, \hat{\mathbf{u}}^{i-1}|u_i)$ ,  $u_i \in \{0, 1\}$  from pairs of channel likelihoods  $W(y_i|x_i)$ ,  $x_i \in \{0, 1\}$ ,  $i \in [0 : N - 1]$ . However, in order to avoid underflows, at each intermediate step of the updates, the likelihoods are scaled by a common factor. Hence scaled versions of the decision likelihoods are eventually computed.

Alternatively, one can avoid such a normalization step by performing the computations in the log-likelihood (LL) domain, i.e., by computing the pairs  $\ln W_n^{(i)}(\mathbf{y}, \hat{\mathbf{u}}^{i-1}[\ell]|u)$ ,  $u \in \{0, 1\}$  for  $i \in [0 : N - 1]$  as a function of channel log-likelihood pairs  $\ln W(y_i|x_i)$ ,  $x_i \in \{0, 1\}$ ,  $i \in [0 : N - 1]$ , as proposed in [10]. Log-likelihoods provide some numerical stability, but still involve some issues compared to the LLRs that we shall discuss in Section V.

Luckily, it turns out that the decoding paths can still be ordered according to their likelihoods using all of the past decision LLRs  $L_n^{(j)}$ ,  $j \in [0 : i]$  and the past trajectory of each path as we shall demonstrate in the following theorem.

**Theorem 2.** *For each path  $\ell \in [0 : L - 1]$  and each level  $i \in [0 : N - 1]$  let the path-metric be defined as:*

$$\text{PM}_\ell^{(i)} \triangleq \sum_{j=0}^i \ln(1 + e^{-(1-2\hat{u}_j[\ell]) \cdot L_n^{(j)}[\ell]}), \quad (11)$$

where

$$L_n^{(i)}[\ell] = \ln \frac{W_n^{(i)}(\mathbf{y}, \hat{\mathbf{u}}^{i-1}[\ell]|0)}{W_n^{(i)}(\mathbf{y}, \hat{\mathbf{u}}^{i-1}[\ell]|1)}$$

is the log-likelihood ratio of bit  $u_i$  given the channel output  $\mathbf{y}$  and the past trajectory of the path  $\hat{\mathbf{u}}^{i-1}[\ell]$ .

If all the information bits are uniformly distributed in  $\{0, 1\}$ , for any pair of paths  $\ell, \ell' \in [0 : L - 1]$ ,

$$W_n^{(i)}(\mathbf{y}, \hat{\mathbf{u}}^{i-1}[\ell]|\hat{u}_i[\ell]) < W_n^{(i)}(\mathbf{y}, \hat{\mathbf{u}}^{i-1}[\ell']|\hat{u}_i[\ell'])$$

if and only if

$$\text{PM}_\ell^{(i)} > \text{PM}_{\ell'}^{(i)}.$$

In view of Theorem 2, one can implement the SCL decoder using  $L$  parallel low-complexity and stable LLR-based SC decoders as the underlying building blocks and, in addition, keep track of  $L$  path-metrics. The metrics can be updated successively as the decoder proceeds according to

$$\text{PM}_\ell^{(i)} = \text{PM}_\ell^{(i-1)} + \ln(1 + e^{-(1-2\hat{u}_i[\ell])L_n^{(i)}[\ell]}). \quad (12)$$

We emphasize that such an update must be performed at *all* indices  $i$  (information and frozen). Any comparison of the likelihoods of the paths can then be done using the values of the path-metrics.

Before proving Theorem 2 let us provide an *intuitive interpretation* of our metric: The SC decoder's decisions (in line 5 of Algorithm 1) would be  $\hat{u}_i = \delta(L_n^{(i)})$  where  $\delta(x) = \frac{1}{2}(1 - \text{sign}(x))$ . Furthermore, since

$$\ln(1 + e^x) \approx \begin{cases} 0 & \text{if } x < 0, \\ x & \text{if } x \geq 0, \end{cases}$$

the update rule (12) is well-approximated as

$$\text{PM}_\ell^{(i)} \approx \begin{cases} \text{PM}_\ell^{(i-1)} & \text{if } \hat{u}_i[\ell] = \delta(L_n^{(i)}[\ell]), \\ \text{PM}_\ell^{(i-1)} + |L_n^{(i)}[\ell]|, & \text{otherwise.} \end{cases} \quad (13)$$

This means that at step  $i$ , if the  $\ell$ -th path does not follow the direction suggested by  $L_n^{(i)}[\ell]$  (i.e., the one that the conventional SC decoder would follow if  $i \in \mathcal{A}$ ), the path will be penalized by an amount of  $\approx |L_n^{(i)}[\ell]|$  (which is the reliability of  $L_n^{(i)}[\ell]$ ).

Having such an interpretation, one might immediately conclude that the path that SC decoder would follow will always have the lowest penalty hence is always declared as the output of the SCL decoder. So why should the SCL decoder exhibit a performance that is better than that of the SC decoder? The answer is that such a reasoning is correct only if *all* the elements of  $\mathbf{u}$  are only information bits. As soon as the decoder encounters a frozen bit, the path metric is updated based on the likelihood of that frozen bit given the past trajectory of the path and the a-priori known value of that bit. This can penalize the SC path by a considerable amount, if the value of that frozen bit does not agree with its LLR given the past trajectory of the path, while keeping some other paths unpenalized.

We devote the rest of this section to prove Theorem 2.

**Lemma 3.** *If  $U_i$  is uniformly distributed in  $\{0, 1\}$ , then,*

$$\frac{W_n^{(i)}(\mathbf{y}, \mathbf{u}^{i-1}|u_i)}{\Pr[\mathbf{U}^i = \mathbf{u}^i | \mathbf{Y} = \mathbf{y}]} = 2 \Pr[\mathbf{Y} = \mathbf{y}].$$

*Proof:* Since  $\Pr[U_i = u_i] = \frac{1}{2}$  for  $\forall u_i \in \{0, 1\}$ ,

$$\begin{aligned} \frac{W_n^{(i)}(\mathbf{y}, \mathbf{u}^{i-1}|u_i)}{\Pr[\mathbf{U}^i = \mathbf{u}^i | \mathbf{Y} = \mathbf{y}]} &= \frac{\Pr[\mathbf{Y} = \mathbf{y}, \mathbf{U}^i = \mathbf{u}^i]}{\Pr[U_i = u_i] \Pr[\mathbf{U}^i = \mathbf{u}^i | \mathbf{Y} = \mathbf{y}]} \\ &= \frac{\Pr[\mathbf{Y} = \mathbf{y}] \Pr[\mathbf{U}^i = \mathbf{u}^i | \mathbf{Y} = \mathbf{y}]}{\Pr[U_i = u_i] \Pr[\mathbf{U}^i = \mathbf{u}^i | \mathbf{Y} = \mathbf{y}]} = 2 \Pr[\mathbf{Y} = \mathbf{y}]. \quad \blacksquare \end{aligned}$$

*Proof of Theorem 2:* We show that

$$\text{PM}_\ell^{(i)} = -\ln(\Pr[\mathbf{U}^i = \hat{\mathbf{u}}^i[\ell] | \mathbf{Y} = \mathbf{y}]) \quad (14)$$

Having shown (14), Theorem 2 will follow as an immediate corollary to Lemma 3 (since the channel output  $\mathbf{y}$  is fixed for all decoding paths). Since the path index  $\ell$  is fixed on both sides of (11) we will drop it in the sequel. Let  $\mu(u) \triangleq 1 - 2u$  and

$$\Lambda_n^{(i)} \triangleq \frac{W_n^{(i)}(\mathbf{y}, \hat{\mathbf{u}}^{i-1}|0)}{W_n^{(i)}(\mathbf{y}, \mathbf{u}^{i-1}|1)} = \frac{\Pr[\mathbf{Y} = \mathbf{y}, \mathbf{U}^{i-1} = \hat{\mathbf{u}}^{i-1}, U_i = 0]}{\Pr[\mathbf{Y} = \mathbf{y}, \mathbf{U}^{i-1} = \hat{\mathbf{u}}^{i-1}, U_i = 1]}$$

(the last equality follows since  $\Pr[U_i = 0] = \Pr[U_i = 1]$ ), and observe that showing (14) is equivalent to proving

$$\Pr[\mathbf{U}^i = \hat{\mathbf{u}}^i | \mathbf{Y} = \mathbf{y}] = \prod_{j=0}^i (1 + (\Lambda_n^{(j)})^{-\mu(\hat{u}_j)})^{-1}. \quad (15)$$

Now we have

$$\begin{aligned} \Pr[\mathbf{Y} = \mathbf{y}, \mathbf{U}^{i-1} = \hat{\mathbf{u}}^{i-1}] &= \sum_{\hat{u}_i \in \{0, 1\}} \Pr[\mathbf{Y} = \mathbf{y}, \mathbf{U}^i = \hat{\mathbf{u}}^i] \\ &= \Pr[\mathbf{Y} = \mathbf{y}, \mathbf{U}^i = \hat{\mathbf{u}}^i] (1 + (\Lambda_n^{(i)})^{-\mu(\hat{u}_i)}) \end{aligned}$$

Therefore,

$$\Pr[\mathbf{Y} = \mathbf{y}, \mathbf{U}^i = \hat{\mathbf{u}}^i] \\ = (1 + (\Lambda_n^{(i)})^{-\mu(\hat{u}_i)})^{-1} \Pr[\mathbf{Y} = \mathbf{y}, \mathbf{U}^{i-1} = \hat{\mathbf{u}}^{i-1}]. \quad (16)$$

Repeated application of (16) (for  $i - 1, i - 2, \dots, 0$ ) yields

$$\Pr[\mathbf{Y} = \mathbf{y}, \mathbf{U}^i = \hat{\mathbf{u}}^i] = \prod_{j=0}^i (1 + (\Lambda_n^{(j)})^{-\mu(\hat{u}_j)})^{-1} \Pr[\mathbf{Y} = \mathbf{y}].$$

Dividing both sides by  $\Pr[\mathbf{Y} = \mathbf{y}]$  proves (15). ■

#### IV. SC DECODER HARDWARE ARCHITECTURE

In the previous section, we saw that the result of Theorem 2 enables the implementation of SCL decoding in the LLR domain. However, before describing our LLR-based SCL decoder architecture, we briefly review the SC decoder architecture of [5], since it performs the crucial task of calculating the path metrics (cf. line 11 of Algorithm 2), thus forming the foundation of our SCL decoder. The SC decoder architecture of [5] consists mainly of three units: the *processing elements* (PEs), the *LLR memory*, and the *partial sums network* (PSN).

##### A. Processing Elements

The PEs compute both the  $\tilde{f}_-$  and the  $f_+$  functions defined in Section II-B4 in a single clock cycle, and the appropriate output is chosen based on a control signal that can be generated based only on the bit index  $i$ . It can be verified that  $N/2$  PEs suffice to achieve maximum intra-stage parallelism [2]. However, it was observed in [5] that by using  $P$  PEs, where  $P \ll N/2$ , the penalty on the decoding latency can be small, while the size of the decoder can be reduced significantly. More specifically, the number of cycles per decoded codeword is given by

$$D_{\text{SC}}(N, P) = 2N + \frac{N}{P} \log \frac{N}{4P}. \quad (17)$$

##### B. LLR Memory and Partial Sum Network

It was shown in [2] that, by employing memory re-use, it suffices to use  $2N - 1$  and  $N - 1$  memory positions to track the  $N \log N$  LLRs and  $\frac{N}{2} \log N$  partial sums that are required during decoding, respectively. Out of the  $2N - 1$  LLRs,  $N$  are *channel* LLRs and  $N - 1$  are *internal* LLRs. Since the PEs require two input LLRs and produce one output LLR, the memory must support simultaneous reads from two distinct memory locations, while at the same time writing to a third memory location. The PSN consists of a  $(N - 1)$ -bit memory, where each memory element is preceded by combinational logic which decides whether each partial sum should be updated with the currently decoded bit  $\hat{u}_i$ .

#### V. SCL DECODER HARDWARE ARCHITECTURE

In this section, we give a detailed description of each unit of our LLR-based SCL decoder architecture, which essentially consists of  $L$  parallel SC decoders along with a path management unit which coordinates the tree search.

Moreover, we highlight its advantages over our previous LL-based architecture described in [10].

Our SCL decoder consists of five units: the *memories unit*, the *metric computation unit* (MCU), the *metric sorting unit*, the *address translation unit*, and the *control unit*. An overview of the SCL decoder is shown in Figure 2.

##### A. LLR and Path Metric Quantization

All LLRs are quantized using a  $Q$ -bit signed uniform quantizer with step size  $\Delta = 1$ . The path metrics are unsigned numbers which are quantized using  $M$  bits. Since the path metrics are initialized to 0 and, in the worst case, they are incremented by  $2^{Q-1} - 1$  for each bit index  $i$ , the maximum possible value of a path metric is  $N(2^{Q-1} - 1) = 2^{n+Q-1} - 2^n \leq 2^{n+Q-1}$ . Hence, at most  $M = n + Q - 1$  quantization bits suffice to ensure that there will be no overflows in the path metric. In practice, any path that gets continuously harshly penalized will most likely be discarded. Therefore, as we will see in Section VII, much fewer bits are sufficient for the quantization of the path metrics.

##### B. Metric Computation Unit

The computation of the path metrics (line 11 of the SCL algorithm in Figure 2) can be fully parallelized. Consequently, the MCU consists of  $L$  parallel SC decoder cores which implement the SC decoding update rules and compute the  $L$  decision LLRs, which are required to update the path metrics  $\text{PM}_\ell^{(i)}$ . Each decoder core reads its input LLRs from one of the  $L$  physical LLR memory banks based on an address translation performed by the pointer memory (described in more detail in Section V-D).

##### C. Memories Unit

1) *LLR Memory*: The channel LLRs are fixed during the decoding process of a given codeword, meaning that an SCL decoder requires only one copy of the channel LLRs. These are stored in a memory which is  $\frac{N}{P}$  words deep and  $QP$  bits wide. On the other hand, the internal LLRs are different for each path  $\ell \in [0 : L - 1]$ . Hence we require  $L$  physical LLR memory banks with  $N - 1$  memory positions per bank. All LLR memories have two reads ports, so that all  $P$  PEs can read their  $Q$ -bit input LLRs simultaneously. The total number of bits used for LLR storage is

$$B_{\text{LLR}} = QN + Q(N - 1)L \lesssim (L + 1)QN. \quad (18)$$

In [5], a regular structure was used for the entire LLR memory, which induces an overhead that diminishes as the block-length grows. This regular structure allowed the authors of [5] to use memory macros, which are more efficient in terms of area. However, the goal of SCL decoding is to avoid very large block-lengths, meaning that the memory overhead of the method proposed in [5] can be significant. For this reason, we use a custom register-based memory as in [2], that can be tailored to the exact number of required bits.

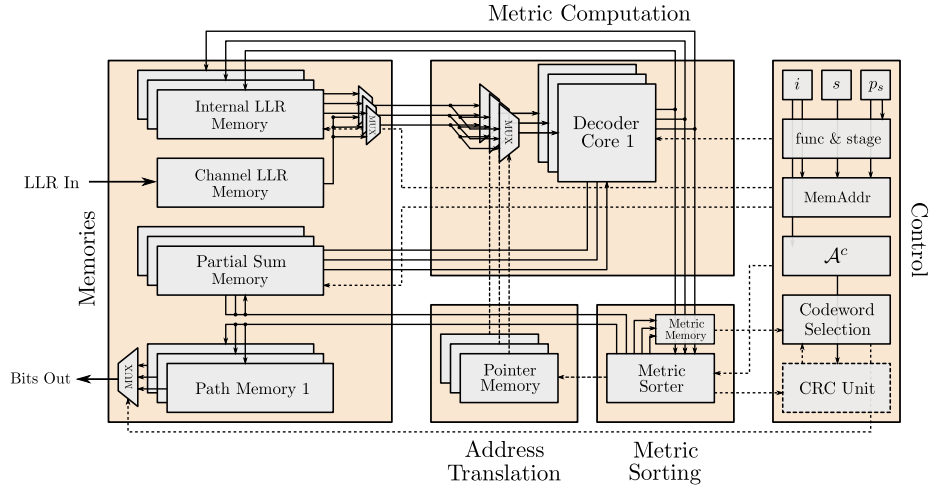


Fig. 2. Overview of the SCL decoder architecture. Details on the  $i, s, p_s$ , as well as the *func & stage* and *MemAddr* components inside the control unit, which are not described in this paper, can be found in [10].

2) *Path Memory*: The path memory consists of  $L$   $N$ -bit registers, denoted by  $\hat{\mathbf{u}}[\ell]$ ,  $\ell \in [0 : L - 1]$ . When a path  $\ell$  needs to be duplicated, the contents of  $\hat{\mathbf{u}}[\ell]$  are copied to  $\hat{\mathbf{u}}[\ell']$ , where  $\ell'$  corresponds to a discarded path. The decoder is stalled for one clock cycle in order to perform the required copying operations by means of  $L \times L$  crossbars which connect each  $\hat{\mathbf{u}}[\ell]$ ,  $\ell \in [0 : L - 1]$  with all other  $\hat{\mathbf{u}}[\ell']$ ,  $\ell' \in [0 : L - 1]$ . After path  $\ell$  has been duplicated, one copy is extended with the bit value  $\hat{u}_i[\ell] = 0$ , while the other is updated with  $\hat{u}_i[\ell'] = 1$  (cf. lines 7 and 19 of Algorithm 2).

3) *Partial Sum Memory*: The partial sum memory consists of  $L$  PSNs. When a path  $\ell \in [0 : L - 1]$  needs to be duplicated, the contents of the PSN  $\ell$  are copied to another PSN  $\ell'$ , where  $\ell'$  corresponds to a discarded path. Copying is performed in a single clock cycle by using  $L \times L$  crossbars which connect each PSN  $\ell \in [0 : L - 1]$  with all other PSNs  $\ell' \in [0 : L - 1]$ . If PSN  $\ell$  was duplicated, one copy is updated with the bit value  $\hat{u}_i[\ell] = 0$ , while the other copy is updated with  $\hat{u}_i[\ell'] = 1$ . If a single copy of PSN  $\ell$  was kept, then this copy is updated with the value of  $\hat{u}_i[\ell]$  that corresponds to the single surviving path.

#### D. Address Translation Unit

The copy-on-write mechanism used in [9] (which is fully applicable to LLRs) is sufficient to ensure that the decoding complexity is  $O(LN \log N)$ , but it is not ideal for a hardware implementation as it still requires copying the LLRs which is costly in terms of power, decoding latency, and silicon area. To this end, a more hardware-friendly solution was proposed in [10], where each path has its own virtual internal LLR memory, the contents of which are physically spread across all of the  $L$  LLR memory banks. Due to the nature of SC decoding, it is possible to store all the LLRs of a given stage in the same memory bank. The translation from virtual memory to physical memory is done using a small *pointer memory*, which tells each of the  $L$  SC decoder cores from which one of the  $L$  memory banks it should read its internal LLRs at each stage  $s \in [0 : n]$ . At stage 0 all SC decoder cores read from

the common channel LLR memory, while the decision LLRs at stage  $n$  do not need to be stored. Therefore, an  $(n - 1) \times L$  memory, denoted by  $\mathbf{P}$ , is sufficient. At decoding stage  $s \in [1 : n - 1]$ , each SC decoder core  $\ell$  reads the contents of  $\mathbf{P}[s, \ell]$  to decide from which physical memory bank it will read its LLRs. Since there are  $L$  memory banks, each entry of  $\mathbf{P}$  can be represented using  $\log L$  bits and the total size of the pointer memory is

$$B_P = L \log L(n - 1) \text{ bits.} \quad (19)$$

When a path  $\ell$  needs to be duplicated, as with the partial sum memory, the contents of row  $\ell$  of the pointer memory are copied to some row corresponding to a discarded path through the use of crossbars.

#### E. Metric Sorting Unit

The metric sorting unit contains a *path metric memory* and a *path metric sorter*. The path metric memory stores the  $L$  path metrics  $\text{PM}_\ell^{(i)}$  using  $M$  bits of quantization for each metric. In order to find the median  $\tau$  for each bit index  $i$  (line 12 of Algorithm 2), the path metric sorter sorts the  $2L$  candidate path metrics  $\text{PM}_\ell^{(i)}$  for  $\hat{u}_i[\ell] \in \{0, 1\}$ . The path metric sorter takes the  $2L$  path metrics as an input and produces the sorted path metrics, as well as the path indices  $\ell$  and bit values  $\hat{u}_i[\ell]$  which correspond to the sorted path metrics as an output. Since decoding can not continue before the surviving paths have been selected, the metric sorter is a crucial component of the SCL decoder. We will discuss the sorter architecture in more detail in Section VI.

#### F. Control Unit

The control unit generates all memory read and write addresses as in [5]. Moreover, the control unit contains the codeword selection unit and the optional CRC unit.

The CRC unit contains  $L$   $r$ -bit CRC memories, which we denote by  $\mathbf{C}[\ell]$ ,  $\ell \in [0 : L - 1]$ , where  $r$  is the number of CRC bits. A bit-serial implementation of a CRC computation unit

is very efficient in terms of area and path delay, but it requires a large number of clock cycles to produce the checksum. However, this computation delay is masked by the bit-serial nature of the SCL decoder itself and, thus, has no impact on the number of clock cycles required to decode each codeword. When decoding of a codeword begins,  $C[\ell]$ ,  $\ell \in [0 : L-1]$  are initialized to the all-zero  $r$ -bit vector. For each  $\hat{u}_i[\ell]$ ,  $i \in \mathcal{A}$ , the CRC unit is activated in order to update the CRC values  $C[\ell]$ . When decoding finishes, the CRC unit declares which paths  $\hat{u}[\ell]$  pass the CRC.

If the CRC unit is present, the codeword selection unit selects the most likely path (i.e., the path with the lowest metric) out of the paths that pass the CRC. Otherwise, the codeword selection unit simply chooses the most likely path.

### G. Clock Cycles Per Codeword

Let the total number of cycles required for metric sorting at all information indices  $i \in \mathcal{A}$  be denoted by  $D_{MS}(\mathcal{A})$ . As we will see in Section VI-C, the sorting latency depends on the number of information bits and may depend on the pattern of frozen and information bits as well (both of these parameters can be deduced given  $\mathcal{A}$ ). Then, our SCL decoder requires

$$D_{SCL}(N, P, \mathcal{A}) = 2N + \frac{N}{P} \log \frac{N}{4P} + D_{MS}(\mathcal{A}) \quad (20)$$

cycles to decode each codeword.

### H. Advantages Over LL-based SCL Decoder Implementation

The LLs in the SCL decoders of [10], [11] are all positive numbers and the corresponding LL-domain update rules involve only additions and comparisons. This means that, as decoding progresses through the decoding stages, the dynamic range of the LLs is increased. Thus, in order to avoid overflows, all LLs in stage  $s$  are quantized using  $Q + s$  bits. In the LLR-based implementation of this paper, the LLRs of all stages are quantized using the same number of bits. This leads to a regular memory where all elements have the same bit-width. Moreover, as we will see in Section VII, using LLRs significantly reduces the total size of the decoder. In addition, the PEs in the LL-based SCL decoder architectures of [10], [11] must support computations with a much larger bit-width than the ones in our LLR-based SCL decoder architecture. Finally, the bit-width of the path metric in the LL-based decoder is significantly larger than the bit-width of the path metric in the LLR-based decoder, increasing the delay and the size of the comparators in the metric sorting unit.

## VI. SIMPLIFIED SORTER

For large list sizes ( $L \geq 4$ ), the maximum delay path passes through the metric sorter, thus reducing the maximum operating frequency of the decoder in [10], [13]. It turns out that the LLR-based path metric we introduced in Theorem 2 has some properties (which the LL-based path metric lacks) that can be used to simplify the sorting task.

To this end, we note that the  $2L$  real numbers that have to be sorted in line 12 of an LLR-based implementation of Algorithm 2 are not arbitrary; half of them are the previously

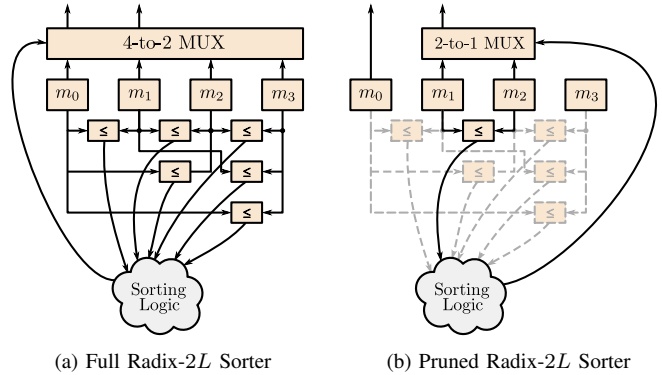


Fig. 3. Radix- $2L$  sorters for  $L = 2$

existing path-metrics (which can be assumed to be already sorted as a result of decoding the preceding information bit) and the rest are obtained by adding positive real values (the absolute value of the corresponding LLRs) to the existing path metrics. Moreover, we do not need to sort *all* these  $2L$  potential path metrics; a sorted list of the  $L$  smallest path metrics is sufficient.

Hence, the sorting task of the SCL decoder can be formalized as follows. Given a sorted list of  $L$  numbers  $\mu_0, \mu_1, \dots, \mu_{L-1}$  (such that  $\mu_\ell \leq \mu_{\ell+1}$  for  $\forall \ell \in [0 : L-2]$ ), a list of size  $2L$ ,  $\mathbf{m} = [m_0, m_1, \dots, m_{2L-1}]$  is created by setting

$$m_{2\ell} := \mu_\ell \quad \text{and} \quad m_{2\ell+1} := \mu_\ell + a_\ell, \quad \ell \in [0 : L-1],$$

where  $a_\ell \geq 0$ , for  $\forall \ell \in [0 : L-1]$ . The problem is to find a sorted list of  $L$  smallest elements of  $\mathbf{m}$  when the elements of  $\mathbf{m}$  have the following two properties: for  $\forall \ell \in [0 : L-2]$ ,

$$m_{2\ell} \leq m_{2(\ell+1)}, \quad (21a)$$

$$m_{2\ell} \leq m_{2\ell+1}. \quad (21b)$$

### A. Full Radix- $2L$ Sorter

The most straightforward way to solve our problem is to sort the list  $\mathbf{m}$  up to the  $L$ -th element. This can be done using a simple extension of the radix- $2L$  sorter described in [16], which blindly compares every pair of elements ( $m_\ell, m_{\ell'}$ ) and then combines the results to find the first  $L$  smallest elements. This is the solution we used in [10], which requires  $\binom{2L}{L} = L(2L-1)$  comparators together with a  $2L$ -to- $L$  multiplexer (see Figure 3a).

The maximum delay of a circuit built based on the radix- $2L$  approach scales in the same way as that of a comparator tree based approach. However, each component in the path of a comparator tree based architecture is a compare-and-select component, while in the radix- $2L$  approach each component is a simple logic gate. Thus, the radix- $2L$  approach results in a smaller maximum delay at the cost of an increased number of comparators with respect to a comparator tree approach (which requires  $4L-1$  comparators). For the small list sizes examined in this work, this additional cost is insignificant compared to the size of the decoder.

## B. Pruned Radix-2L Sorter

The full radix-2L sorter carries out too many comparisons since we already know the result of some of the pairwise comparisons. Furthermore, the results of some of comparisons are not needed because we do not need to sort the entire list  $\mathbf{m}$ . Therefore, we can *prune* the radix-2L sorter by removing these unnecessary comparators.

**Proposition 4.** *It is sufficient to use a pruned radix-2L sorter that involves only  $(L-1)^2$  comparators to get the  $L$  smallest elements of  $\mathbf{m}$ . This sorter is obtained by*

- (a) *removing the comparisons between every even-indexed element of  $\mathbf{m}$  and all following elements, and*
- (b) *removing the comparisons between  $m_{2L-1}$  and all other elements of  $\mathbf{m}$ .*

*Proof:* Properties (21a) and (21b) imply  $m_{2\ell} \leq m_{\ell'}$  for  $\forall \ell' > 2\ell$ . Hence, the outputs of these comparators are known. Furthermore, as we only need the first  $L$  elements of the list sorted and  $m_{2L-1}$  is never among the  $L$  smallest elements of  $\mathbf{m}$ , we can always replace  $m_{2L-1}$  by  $+\infty$  (pretending the result of the comparisons involving  $m_{2L-1}$  is known) without affecting the output of the sorter.

In step (a) we have removed  $\sum_{\ell=0}^{L-1} (2L-1-2\ell) = L^2$  comparators and in step (b)  $(L-1)$  comparators (note that in the full sorter  $m_{2L-1}$  is compared to all  $(2L-1)$  preceding elements but  $L$  of them correspond to even-indexed elements whose corresponding comparators have already been removed in step (a)). Hence we have  $L(2L-1) - L^2 - (L-1) = (L-1)^2$  comparators. ■

Besides the  $(L-1)^2$  comparators, the pruned radix-2L sorter requires a  $(2L-2)$ -to- $(L-1)$  multiplexer (see Figure 3b). This reduction significantly reduces the maximum delay of the corresponding circuit since a large number of logic gates can be removed from the critical path.

The pruned radix-2L sorter is derived based on the assumption that the existing path metrics are already sorted. This assumption is violated when the decoder reaches the first frozen bit after the first cluster of information bits; at each frozen index, some of the path-metrics are unchanged and some are increased by an amount equal to the absolute value of the LLR. In order for the assumption to hold when the decoder reaches the next cluster of information bits, the  $L$  existing path metrics have to be sorted before the decoding of this cluster starts.

Fortunately, it turns out that the existing pruned radix-2L sorter can be used for sorting  $L$  arbitrary positive numbers as follows.

**Proposition 5.** *Let  $\mathbf{a} = [a_0, a_1, \dots, a_{L-1}]$  be a list of size  $L$  of non-negative numbers. Create a list of size  $2L$  as*

$$\mathbf{b} = [0, a_0, 0, a_1, \dots, 0, a_{L-2}, a_{L-1}, +\infty].$$

*Feeding this list to the pruned radix-2L sorter will result in an output list of the form*

$$\underbrace{[0, 0, \dots, 0]}_{L-1 \text{ zeros}}, a'_0, a'_1, \dots, a'_{L-1}, +\infty$$

*where  $\langle a'_0, a'_1, \dots, a'_{L-1} \rangle$  is the sorted version of  $\mathbf{a}$ .*

*Proof:* It is clear that the assumptions (21a) and (21b) hold for  $\mathbf{b}$ . The proof of Proposition 4 shows if the last element of the list is additionally known to be the largest element, the pruned radix-2L sorter sorts the entire list. ■

We note that while the same comparator network of a pruned radix-2L sorter is used for sorting  $L$  numbers, a different  $L$ -to- $L$  multiplexer is required to output the sorted list.

## C. Latency of Metric Sorting

We assume that the sorting procedure is carried out in a single clock cycle. A decoder based on the full radix-2L sorter, only needs to sort the path metrics for the information indices, hence, the total sorting latency of such an implementation is

$$D_R(\mathcal{A}) = |\mathcal{A}| = NR \text{ cycles.} \quad (22)$$

Using the pruned radix-2L sorter, additional sorting steps are required at the end of each contiguous set of frozen indices. Let  $F_C(\mathcal{A})$  denote the number of *clusters* of frozen bits for a given information set  $\mathcal{A}$ .<sup>4</sup> The metric sorting latency using the pruned radix-2L sorter is

$$D_{PR}(\mathcal{A}) = |\mathcal{A}| + F_C(\mathcal{A}) = NR + F_C(\mathcal{A}) \text{ cycles.} \quad (23)$$

## VII. IMPLEMENTATION RESULTS

In this section, we present synthesis results for our SCL decoder architecture. For fair comparison with [11], we use a TSMC 90 nm technology with a typical timing library (1 V supply voltage, 25°C operating temperature) and our decoder of [10] is re-synthesized using this technology. All synthesis runs are performed with timing constraints that are not achievable, in order to assess the maximum achievable operating frequency of each design, as reported by the synthesis tool. For our synthesis results, we have used  $P = 64$  PEs per SC decoder core, as in [5], [10].

We first compare the LLR-based decoder of this work with our previous LL-based decoder [10], in order to demonstrate the improvements obtained by moving to an LLR-based formulation of SCL decoding. Then, for completeness, we also compare our LLR-based decoder with the LL-based decoder of [11]. A direct comparison with the decoder of [12] is unfortunately not possible, as the authors do not provide synthesis results. Finally, we provide some discussion on the effectiveness of a CRC-aided SCL decoder.

### A. Quantization Parameters

In Figure 4, we present the FER of floating-point and fixed-point implementations of an LL-based and an LLR-based SCL decoder for a polar code of length  $N = 1024$  and rate  $R = 1/2$ .<sup>5</sup> For the floating-point simulations we have used the

<sup>4</sup> More precisely we assume  $\mathcal{F} = \bigcup_{j=1}^{F_C(\mathcal{A})} \mathcal{F}_j$  such that (i)  $\mathcal{F}_j \cap \mathcal{F}_{j'} = \emptyset$  if  $j \neq j'$ , i.e.,  $\{\mathcal{F}_j, j = 1, \dots, F_C(\mathcal{A})\}$  is a partition of  $\mathcal{F}$ ; (ii) for every  $j$ ,  $\mathcal{F}_j$  is a contiguous subset of  $[0 : N-1]$ ; and (iii) for every pair  $j \neq j'$ ,  $\mathcal{F}_j \cup \mathcal{F}_{j'}$  is *not* a contiguous subset of  $[0 : N-1]$ . It can be easily checked that such a partition always exists and is unique.

<sup>5</sup>The code is optimized for  $E_b/N_0 = 2\text{dB}$  and constructed using the Monte-Carlo method of [1, Section IX].

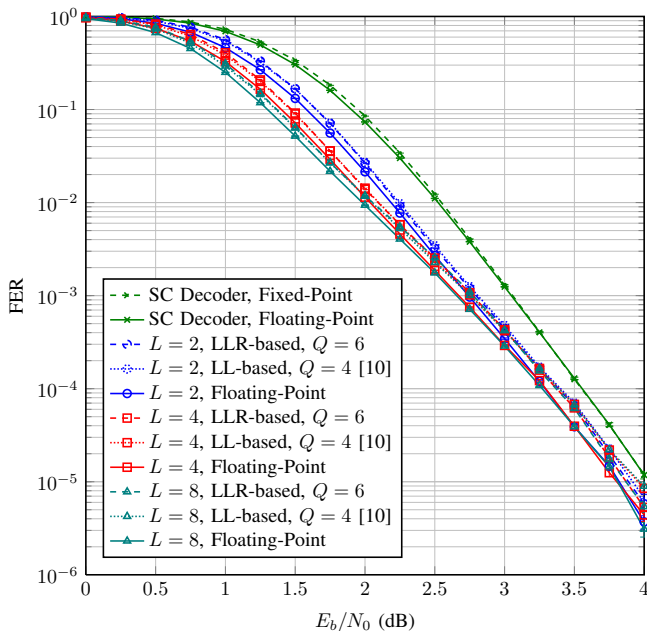


Fig. 4. The performance of floating-point versus fixed-point SCL decoders.

exact implementation of the decoder, i.e., for computing the LLRs the update rule  $f_-$  of (8a) is used and the path metric is iteratively updated according to (12). In contrast, for the fixed-point simulations we have used the min-sum approximation of the decoder (i.e., replaced  $f_-$  with  $\hat{f}_-$  as in (10)) and the approximated path metric update rule of (13).

We observe that the LL-based and the LLR-based SCL have practically indistinguishable FER performance when quantizing the channel LLs and the channel LLRs with  $Q = 4$  bits and  $Q = 6$  bits, respectively. Moreover, in our simulations we observe that the performance of the LL and the LLR-based SCL decoder is degraded significantly when  $Q < 6$  and  $Q < 4$ , respectively. As discussed in Section V-A, metric quantization requires at most  $M = n + Q - 1$  bits. However, in practice, much fewer bits turn out to be sufficient. For example, in our simulations for  $N = 1024$  and  $Q = 6$ , setting  $M = 8$  leads to the same performance as the worst-case  $M = 15$ , while setting  $M = 7$  results in a significant performance degradation due to metric saturation. Thus, all synthesis results of this section are obtained for  $Q = 4$  for the LL-based decoder of [10], and  $Q = 6$  and  $M = 8$  for the LLR-based decoder for a fair (i.e., iso-FER) comparison.

The authors of [11] only provide the FERs for a CRC-aided SCL decoder [11, Figure 3]. Nevertheless, we believe since they implement exactly the same algorithm as in [10] (using a different *architecture* than [10]), their quantization scheme will not result in a *better* FER performance for a *standard* SCL decoder than that of [10].

## B. LL-Based Decoders vs. LLR-Based SCL Decoder

1) *Comparison with [10]*: Our previous LL-based architecture of [10] and the LLR-based architecture with a radix-2L sorter presented in this paper are almost identical. The only difference is the use of LLs and LLRs, respectively. Therefore,

TABLE I  
CELL AREA BREAKDOWN FOR THE LL-BASED AND THE RADIX-2L  
LLR-BASED SCL DECODERS ( $R = \frac{1}{2}$ ,  $N = 1024$ )

	LL-Based [10]	LLR-Based	Reduction
List Size	$L = 2$		
Total Area (mm <sup>2</sup> )	1.38	0.88	36%
Memory (mm <sup>2</sup> )	1.07	0.80	25%
MCU (mm <sup>2</sup> )	0.28	0.06	79%
Metric Sorter (mm <sup>2</sup> )	$1.34 \times 10^{-3}$	$0.75 \times 10^{-3}$	44%
Other (mm <sup>2</sup> )	0.03	0.02	50%
List Size	$L = 4$		
Total Area (mm <sup>2</sup> )	2.62	1.75	33%
Memory (mm <sup>2</sup> )	1.92	1.57	18%
MCU (mm <sup>2</sup> )	0.54	0.11	80%
Metric Sorter (mm <sup>2</sup> )	$13.92 \times 10^{-3}$	$9.23 \times 10^{-3}$	33%
Other (mm <sup>2</sup> )	0.15	0.06	60%
List Size	$L = 8$		
Total Area (mm <sup>2</sup> )	5.38	3.87	28%
Memory (mm <sup>2</sup> )	4.08	3.46	15%
MCU (mm <sup>2</sup> )	0.82	0.18	78%
Metric Sorter (mm <sup>2</sup> )	$70.65 \times 10^{-3}$	$54.05 \times 10^{-3}$	24%
Other (mm <sup>2</sup> )	0.41	0.18	56%

by comparing these two architectures we can identify the improvements in terms of area, and decoding throughput that arise directly from the reformulation of SCL decoding in the LLR domain.

From Table I, we see that our LLR-based SCL decoder occupies 36%, 33%, and 28% smaller area than our LL-based SCL decoder of [10] for  $L = 2$ ,  $L = 4$ , and  $L = 8$ , respectively. In Table I, we present the area breakdown of the LL-based and the LLR-based decoders. We observe that, in absolute terms, the most significant savings in terms of area come from the memory, where the area is reduced by up to 0.62 mm<sup>2</sup> for  $L = 8$ . On the other hand, in relative terms, the biggest savings in terms of area come from the MCU with an average area reduction of 79%.

In Table II we present decoding throughput and *hardware efficiency* (throughput per unit area) of our LLR-based decoder and the LL-based decoders of [10], [11]. The decoding throughput of all decoders is calculated as

$$T_{\text{SCL}}(N, P, \mathcal{A}, f) = \frac{f \cdot N}{D_{\text{SCL}}(N, P, \mathcal{A})}, \quad (24)$$

where  $f$  is the operating frequency of the decoder.

The cycle count for the radix-2L sorter when using a polar code of rate  $R = 1/2$  and length  $N = 1024$  is  $D_{\text{R}}(\mathcal{A}) = |\mathcal{A}| = 512$  cycles, so that  $D_{\text{SCL}}(N, P, \mathcal{A}) = 2592$  cycles. As we will see in Section VII-C, the cycle count of the pruned radix-2L sorter is slightly higher. From Table II, we observe that the operating frequency and, consequently, the throughput of our radix-2L LLR based decoder is 7%, 3%, and 2% higher than that of our LL-based SCL decoder of [10] for  $L = 2$ ,  $L = 4$ , and  $L = 8$ , respectively.

Due to the aforementioned improvements in area and decoding throughput, the LLR-based formulation of SCL decoding leads to hardware decoders with 67%, 55%, and 40% better hardware efficiency than the corresponding LL-based decoders of [10], for  $L = 2$ ,  $L = 4$ , and  $L = 8$ , respectively.

2) *Comparison with [11]*: From Table II we observe that our radix-2L LLR-based SCL decoder has a 58%, 57%, and

TABLE II  
SCL DECODER SYNTHESIS RESULTS ( $R = \frac{1}{2}$ ,  $N = 1024$ )

	LL-Based [11]*			LL-Based [10]			LLR-Based					
	$L = 2$	$L = 4$	$L = 8$	$L = 2$	$L = 4$	$L = 8$	Radix-2L Sorter			Pruned Radix-2L Sorter		
							$L = 2$	$L = 4$	$L = 8$	$L = 2$	$L = 4$	$L = 8$
Frequency (MHz)	800	632	625	794	730	408	847	758	415	848	794	637
Throughput (Mbits/s)	319	208	177	314	287	160	335	300	164	328	307	246
Cell Area (mm <sup>2</sup> )	2.11	4.03	8.64	1.38	2.62	5.38	0.88	1.75	3.87	0.90	1.78	3.85
Efficiency (Mbits/s/mm <sup>2</sup> )	151	52	20	228	110	30	381	171	42	364	172	64

\* The synthesis results in [11] are provided with  $Q = 3$  quantization bits for the list sizes  $L = 2$  and  $L = 4$ . The reported numbers in this table are the corresponding synthesis results using  $Q = 4$  and are courtesy of the authors of [11].

55% smaller area than the LL-based SCL decoder of [11] for  $L = 2$ ,  $L = 4$ , and  $L = 8$ , respectively. It is not surprising that the improvement in area with respect to the architecture of [11] is larger than the improvement in area with respect to the architecture of [10], since the authors of [11] instantiate an  $L \times L$  crossbar to copy each of the  $2N - 1$  LLs, while these crossbars have been eliminated in [10].

Moreover, the throughput of our LLR-based SCL decoder is 5% and 44% higher than the throughput achieved by the LL-based SCL decoder of [11] for  $L = 2$  and  $L = 4$ , respectively. However, for  $L = 8$  our decoder is 7% slower. This happens because the pipelined bitonic metric sorter used in [11] scales better with the list size  $L$ , leading to a higher operating frequency and an overall increased throughput. As we will demonstrate with the results in Section VII-C, we can solve this issue by using the pruned radix-2L sorter.

Nevertheless, the hardware efficiency of our LLR-based SCL decoder is still 152%, 229%, and 110% higher than that of [11] for  $L = 2$ ,  $L = 4$  and  $L = 8$ , respectively.

### C. Radix-2L Sorter vs. Pruned Radix-2L Sorter

One may expect the pruned radix-2L sorter to always outperform the radix-2L sorter, as it has lower area and a shorter maximum path delay. Recall, however, that the decoder equipped with the pruned radix-2L sorter needs to stall slightly more often. More specifically, a polar code of rate  $R = 1/2$  and length  $N = 1024$  contains  $F_C(\mathcal{A}) = 57$  groups of frozen bits. Therefore, the total sorting latency for the pruned radix-2L sorter is  $D_{PR}(\mathcal{A}) = |\mathcal{A}| + F_C(\mathcal{A}) = 569$  cycles. Thus, we have  $D_{SCL}(N, P, \mathcal{A}) = 2649$  cycles, which is an increase of approximately 2% with respect to the decoder equipped with a full radix-2L sorter. Therefore, if using the pruned radix-2L does not lead to a more than 2% higher clock frequency, the decoding throughput will actually be lowered.

As can be observed in Table II, this is exactly the case for  $L = 2$ , where the LLR-based SCL decoder with the pruned radix-2L sorter has a 2% lower throughput than the LLR-based SCL decoder with the full radix-2L sorter. For  $L = 2$ , the metric sorter does not lie on the critical path of the decoder. Thus, using the decoder with the pruned radix-2L sorter does not achieve a higher operating frequency than the decoder with the radix-2L sorter. However, for  $L \geq 4$  the metric sorter does lie on the critical path of the decoder, so using the pruned radix-2L sorter results in a significant increase in throughput of up to 50% for  $L = 8$ .

If we now compare the decoder of [11] for  $L = 8$  with our pruned radix-2L LLR-based decoder, we see that our

decoder can achieve a 39% higher throughput, leading to a 220% higher hardware efficiency. Moreover, if we do the same comparison with our LL-based decoder of [10], we observe 54% increase in the throughput and 113% gain in hardware efficiency.

### D. CRC-Aided SCL Decoder

As discussed in Section II-D, the performance of the SCL decoder can be significantly improved if it is assisted for its final choice by means of a CRC which rejects some incorrect codewords from the final set of  $L$  candidates. However, there is a trade-off between the length of the CRC and the performance gain. The longer the CRC, the more incorrect codewords it can reject. On the other side, adding  $r$  CRC bits degrades the performance of the inner polar code due to the increase in its rate. Hence, the CRC improves the overall performance if the performance degradation of the inner polar code is compensated by means of rejecting the incorrect codewords in the final list.

1) *Choice of CRC*: We picked three different CRCs of lengths  $r = 4$ ,  $r = 8$  and  $r = 16$  from [17] with generator polynomials:

$$g(x) = x^4 + x + 1, \quad (25a)$$

$$g(x) = x^8 + x^7 + x^6 + x^4 + x^2 + 1, \text{ and} \quad (25b)$$

$$g(x) = x^{16} + x^{15} + x^2 + 1, \quad (25c)$$

respectively and evaluated the empirical performance of the SCL decoders of list sizes of  $L = 2$ ,  $L = 4$ ,  $L = 8$ , aided by each of these three CRCs in the regime of  $E_b/N_0 = 0$  dB to  $E_b/N_0 = 4$  dB.

For  $L = 2$  it turns out that the smallest CRC, represented by the generator polynomial in (25a), is the best choice. Using longer CRCs at moderate SNR regime, the performance degradation of the polar code is more significant, causing the CRC-aided SCL decoder to perform worse than the standard SCL decoder. Furthermore, in high-SNR regime, longer CRCs does not lead to a better performance than the CRC-4.

For  $L = 4$ , allocating  $r = 8$  bits for the CRC of (25b) turns out to be the most beneficial option. CRC-8 improves the FER significantly more than CRC-4, while CRC-16 leads to the same performance as CRC-8 at high SNRs and worse performance than CRC-8 in moderate SNR regime.

Finally, for  $L = 8$  we observe that CRC-16 of (25c) is the best candidate among the three different CRCs in the sense that the performance of the CRC-aided SCL decoder which uses this CRC is significantly better than that of the decoders

using CRC-4 or CRC-8 for  $E_b/N_0 > 2.5$  dB, while all three decoders have almost the same FER at lower SNRs (and they all perform better than a standard SCL decoder).

In Figure 5, we compare the FER of the SCL decoder with that of the CRC-aided SCL decoder for list sizes of  $L = 2$ ,  $L = 4$  and  $L = 8$ , using the above-mentioned CRCs. We observe that the CRC-aided SCL decoders perform significantly better than the standard SCL decoders.

2) *Throughput Reduction*: Adding  $r$  bits of CRC increases the number of information bits by  $r$ , while reducing the number of groups of frozen channels by *at most*  $r$ . As a result, the sorting latency is generally increased, resulting in a decrease in the throughput of the decoder. In Table III we have computed this decrease in the throughput for different decoders and we see that the CRC-aided SCL decoders have slightly (at most 0.4%) reduced throughput. For this table, we have picked the best decoder at each list size in terms of hardware efficiency from Table II. That is to say, for  $L = 2$  we have used the SCL decoder with radix- $2L$  sorter and for the other two list sizes we have used the SCL decoder with pruned radix- $2L$  sorter.

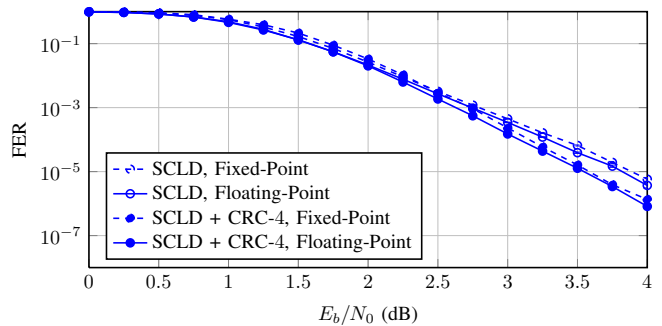
TABLE III  
THROUGHPUT REDUCTION IN CRC-AIDED SCL DECODERS

		$L = 2$	$L = 4$	$L = 8$
Freq. (MHz)		847	794	637
SCLD	$ \mathcal{A} $	512	512	512
	$F_C(\mathcal{A})$	57	57	57
	$D_{SCL}$	2592	2649	2649
	T/P (Mbits/s)	335	307	246
CRC-Aided SCLD	$ \mathcal{A} $	516	520	528
	$F_C(\mathcal{A})$	55	54	52
	$D_{SCL}$	2596	2654	2660
	T/P (Mbits/s)	334	306	245
Reduction (%)		0.2	0.2	0.4

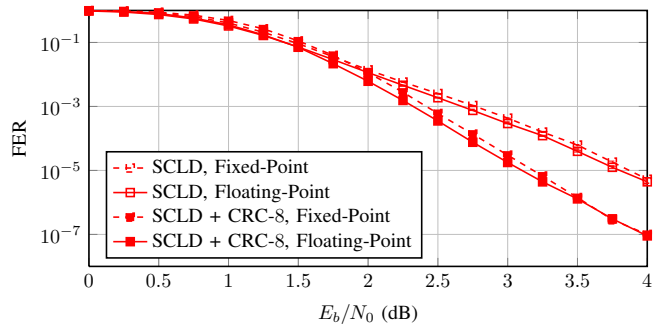
3) *Effectiveness of CRC*: The area of the CRC unit for all synthesized decoders is in the order of  $10^{-6}$  mm<sup>2</sup> for the employed TSMC 90 nm technology. Moreover, the CRC unit does not lie on the critical path of the decoder. Therefore, it does not affect the maximum achievable operating frequency. Thus, if the best possible FER performance is of the greatest concern, the incorporation of a CRC unit is a highly effective method of improving the performance of an SCL decoder. For example, it is interesting to note that the CRC-aided decoder with  $L = 2$  has a somewhat lower FER than the standard SCL decoder with  $L = 8$  (for both the floating-point and the fixed-point versions) in the regime of  $E_b/N_0 > 2.5$  dB. Therefore, if a FER in the range of  $10^{-3}$  to  $10^{-6}$  is required by the application, using a CRC-aided SCL decoder with list size  $L = 2$  is preferable to a standard SCL decoder with list size  $L = 8$  as the former has six times higher hardware efficiency.

## VIII. CONCLUSION

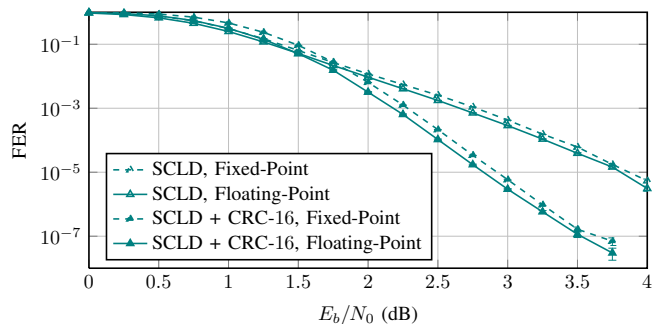
In this work, we introduced an LLR-based path metric for SCL decoding of polar codes, which enables the implementation of a numerically stable LLR-based SCL decoder. Moreover, we showed that we can simplify the sorting task of the SCL decoder by using a pruned radix- $2L$  sorter which exploits the properties of the LLR-based path metric. The



(a)  $L = 2$



(b)  $L = 4$



(c)  $L = 8$

Fig. 5. Comparison of floating-point and fixed-point LLR-based SCL decoders with CRC-Aided SCL decoders for  $L = 2, 4, 8$ .

LLR-based path metric is not specific to SCL decoding and can be applied to any other tree-search based decoder (e.g., stack SC decoding [14]).

Finally, we implemented a hardware architecture for an LLR-based SCL decoder and we presented synthesis results for various list sizes. Our synthesis results clearly show that our LLR-based SCL decoder has a significantly higher throughput *and* lower area than all existing decoders in the literature, leading to a substantial increase in hardware efficiency of up to 220%.

## REFERENCES

- [1] E. Arıkan, "Channel polarization: A method for constructing capacity-achieving codes for symmetric binary-input memoryless channels," *IEEE Transactions on Information Theory*, vol. 55, no. 7, pp. 3051–3073, Jul. 2009.
- [2] C. Leroux, I. Tal, A. Vardy, and W. J. Gross, "Hardware architectures for successive cancellation decoding of polar codes," in *Proceedings of 2011 IEEE International Conference on Acoustics, Speech and Signal Processing (ICASSP)*, May 2011, pp. 1665–1668.

- [3] A. J. Raymond and W. J. Gross, "Scalable successive-cancellation hardware decoder for polar codes," in *Proceedings of 2013 IEEE Global Conference on Signal and Information Processing (GlobalSIP)*, Dec. 2013, pp. 1282–1285.
- [4] A. Pamuk and E. Arkan, "A two phase successive cancellation decoder architecture for polar codes," in *Proceedings of IEEE International Symposium on Information Theory (ISIT)*, Jul. 2013, pp. 957–961.
- [5] C. Leroux, A. J. Raymond, G. Sarkis, and W. J. Gross, "A semi-parallel successive-cancellation decoder for polar codes," *IEEE Transactions on Signal Processing*, vol. 61, no. 2, pp. 289–299, Jan. 2013.
- [6] C. Zhang and K. K. Parhi, "Low-latency sequential and overlapped architectures for successive cancellation polar decoder," *IEEE Transactions on Signal Processing*, vol. 61, no. 10, pp. 2429–2441, Mar. 2013.
- [7] A. Mishra, A. J. Raymond, L. Amaru, G. Sarkis, C. Leroux, P. Meinerzhagen, A. Burg, and W. J. Gross, "A successive cancellation decoder ASIC for a 1024-bit polar code in 180nm CMOS," in *Proceedings of 2012 IEEE Asian Solid State Circuits Conference (A-SSCC)*, Nov. 2012, pp. 205–208.
- [8] E. Arkan and E. Telatar, "On the rate of channel polarization," in *Proceedings of IEEE International Symposium on Information Theory (ISIT)*, 2009, Jul. 2009, pp. 1493–1495.
- [9] I. Tal and A. Vardy, "List decoding of polar codes," in *Proceedings of IEEE International Symposium on Information Theory (ISIT)*, 2011, Jul. 2011, pp. 1–5.
- [10] A. Balatsoukas-Stimming, A. J. Raymond, W. J. Gross, and A. Burg, "Hardware architecture for list successive cancellation decoding of polar codes," *IEEE Transactions on Circuits and Systems II: Express Briefs*, vol. 61, no. 8, May 2014.
- [11] J. Lin and Z. Yan, "Efficient list decoder architecture for polar codes," in *Proceedings of IEEE International Symposium on Circuits and Systems (ISCAS)*, Jun. 2014, pp. 1022–1025.
- [12] C. Zhang, X. You, and J. Sha, "Hardware architecture for list successive cancellation polar decoder," in *Proceedings of IEEE International Symposium on Circuits and Systems (ISCAS)*, Jun. 2014, pp. 209–212.
- [13] A. Balatsoukas-Stimming, M. Bastani Parizi, and A. Burg, "LLR-based successive cancellation list decoding of polar codes," in *Proceedings of 2014 IEEE International Conference on Acoustics, Speech and Signal Processing (ICASSP)*, May 2014, pp. 3903–3907.
- [14] K. Chen, K. Niu, and J. Lin, "Improved successive cancellation decoding of polar codes," *IEEE Transactions on Communications*, vol. 61, no. 8, pp. 3100–3107, Aug. 2013.
- [15] F. J. MacWilliams and N. J. A. Sloane, *The Theory of Error Correcting Codes*, ser. North-Holland Mathematical Library. North-Holland, 1978.
- [16] L. G. Amaru, M. Martina, and G. Masera, "High speed architectures for finding the first two maximum/minimum values," *IEEE Transactions on Very Large Scale Integration Systems*, vol. 20, no. 12, pp. 2342–2346, Dec. 2012.
- [17] Wikipedia. (2014, Sep.) Polynomial representations of cyclic redundancy checks — wikipedia, the free encyclopedia. [Online]. Available: [http://en.wikipedia.org/w/index.php?title=Polynomial\\_representations\\_of\\_cyclic\\_redundancy\\_checks&oldid=620254949](http://en.wikipedia.org/w/index.php?title=Polynomial_representations_of_cyclic_redundancy_checks&oldid=620254949)